

Detailed Measurements of Inelastic Scattering in Anderson Localization

Shanjin He and J. D. Maynard

Department of Physics, The Pennsylvania State University, University Park, Pennsylvania 16802

(Received 26 September 1986)

Considerable progress has been made in the experimental observation of Anderson localization and quantum eigenstate coherence for electrons in disordered solids. The coherence effects deduced from conductivity measurements require some corrections for inelastic scattering, and often the necessary information is imprecisely known. In this Letter we report detailed observations of inelastic effects in an acoustic localization experiment where parameters may be precisely controlled and measured; some phase-correlation effects are evident.

PACS numbers: 43.20.+g, 71.55.Jv

As a consequence of Bloch's theorem, the eigenstates of a system described by a periodic potential are extended, having the same nominal amplitude at all positions in space. When a random element is added to the potential field, the eigenstate amplitude may not simply acquire a random variation but may instead become localized, decaying exponentially from a particular site with a characteristic length. This phenomenon, originally discussed by Anderson¹ and Mott,² is interesting not only as an unusual consequence of disorder, but also because it can be used to reflect the coherence of electron quantum states in solids. The Anderson localization effects are strongest in one-dimensional systems, and there has been considerable experimental effort devoted to the observation of clear effects for electrons in narrow wires and semiconductor channels.^{3,4} The experimental problems are formidable, for one must contend with the effects of thermal broadening of the electron energy, the quasi one-dimensionality of the system, etc., and one must eliminate or at least separate various inelastic processes which weaken the eigenstate coherence. Considerable progress has been made, with experiments probing fewer electron eigenstates with less confusion, but still some corrections for inelastic effects are necessary, and often the required information is imprecisely known. It is possible to observe localization effects in other wave systems, such as ones involving photons,⁵ phonons,⁶ or quantum-fluid waves,⁷ where observations may be more straightforward. We have been making such measurements in an acoustic localization experiment where we can observe in detail eigenstate amplitude and phase, eigenvalue spectra and density of states, and dependence of localization length on strength of disorder, showing fluctuations⁸ as a function of position within a band, separation from nearby states, etc. Recently we have made measurements of the effect of inelastic scattering, which, involving an extended time-dependent potential,⁹ is not easily determined with analytic or numerical computation. In this Letter we present detailed measurements of the transfer of energy from one localized eigenstate to another (phonon-assisted hopping), in the presence of a

well-defined inelastic process. Our results indicate that estimates based only on the overlap of the amplitude of the eigenstates¹⁰ cannot fully account for the variation in the hopping probability.

The analogy between electron-wave and acoustic-wave localization has been discussed in the literature.^{6,11} The wave functions ψ may be superpositions of energy states with time dependence $\exp(iEt/\hbar)$ for electrons, or monotonal waves with time dependence $\exp(i\omega t)$ for sound waves. For these states the wave equation may be written

$$\nabla^2\psi + [q^2 - V(r)]\psi = 0, \quad (1)$$

where for particles $q^2 = 2mE/\hbar^2$ (with m the particle mass), and for sound waves $q = \omega/C$ (with C the characteristic speed of sound). $V(r)$ is the potential (normalized with $2m/\hbar^2$) for particles and a combination of a stiffness operator and mass density for an acoustic medium. For a one-dimensional acoustic system V is easily determined from basic mechanics or acoustics.

The one-dimensional acoustic system used in our experiments is illustrated in Fig. 1. The wave medium is a long (15 m), 0.17-mm-diam steel wire suspended vertically; a tension T in the wire is maintained by a spring attached at the lower end. The wave field ψ consists of transverse waves in the wire generated with an electromechanical actuator at one end of the wire. The periodic or nearly periodic potential field V for the wire is provided by small lead masses (with mass $m = 249 \pm 33$ mg) spaced along the wire with an average lattice constant $a = 15$ cm; a total of fifty masses are used. The masses are sufficiently small that the potential V may be approximated as a series of delta functions with strength $m\omega^2/T$. Experimental measurements and computer simulations have shown that the small variations in the size of the masses have negligible effects on the phenomena which we study, as will be discussed later.

Beyond the series of masses the wire continues for a few meters and is then covered with a long taper of cotton which provides an anechoic termination. Running parallel to the wire is a 9-m aluminum beam which acts

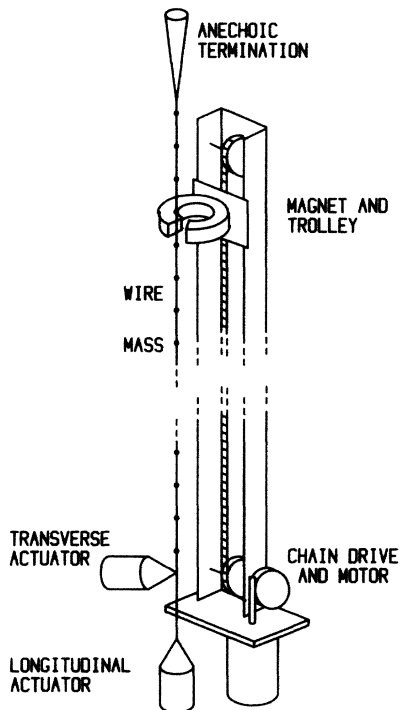


FIG. 1. One-dimensional acoustic Anderson localization experiment.

as a guide for a trolley carrying a C-shaped permanent magnet. The magnet is aligned so that the wire passes between its poles, with the lines of force perpendicular to the wire. When the transverse wave field is present along the wire, the magnetic field induces an emf in the wire which is proportional to the velocity of the wire at the position of the magnet. The emf is measured by the grounding of one end of the wire and connection of the opposite end (through a fine copper wire) to a preamplifier and two-phase lock-in amplifier referenced to the transverse actuator signal. A motor, gear, and chain system is used to translate the trolley and magnet assembly along the aluminum beam. By monitoring of the position of the magnet and the current induced in the wire, the entire wave field along the wire, including amplitude and phase, may be recorded.

If one considers an electron wave in a one-dimensional potential as being represented by the transverse wave in the wire-mass system, then an electron-phonon interaction may be simulated by modulation of the longitudinal strain in the wire. That is, for low-frequency (essentially zero wave vector) phonons, the electron-phonon interaction may be modeled by replacement of the potential $V(r)$ in Eq. (1) by $V(r + r\epsilon \cos \Omega t)$ where $\epsilon \cos \Omega t$ is the strain field of a phonon of frequency Ω .¹² In our experiment the longitudinal strain is modulated directly with a second electromechanical actuator at the end of the wire, as shown in Fig. 1. By driving the longitudinal actuator

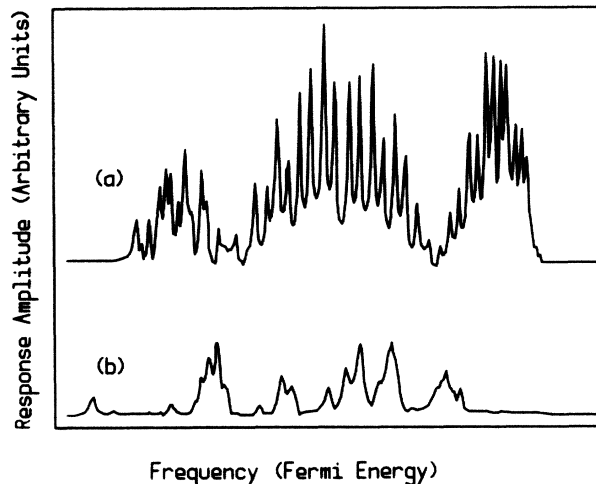


FIG. 2. Response of the wire at one end as a function of the frequency of the transverse actuator at the opposite end (analogous to electron Fermi energy in a conductivity experiment). (a) Periodic potential. (b) 2% random potential.

with a synthesized "thermal phonon" spectrum, we could simulate finite-temperature effects. However, in order to study an isolated inelastic-scattering process in detail, we use only a single frequency Ω , providing the well-defined time-dependent potential $V(r + r\epsilon \cos \Omega t)$.

In the wire-mass system disorder may be introduced by variation of the sizes of the masses (alloy-type disorder) or by variation of the positions of the masses (liquid-type disorder).¹³ We found that the liquid-type disorder, even for very small deviations from periodicity, produced more dramatic localization effects. For example, variation of the positions of the masses by less than 1% produced significant localization, while the inherent $\sim 13\%$ variation in the sizes of the commercial lead masses resulted in localization lengths which were much larger than the size of our system. For experimental convenience we varied the positions of the masses; several sets of measurements were made with the positions randomly varied within maximum displacements from lattice sites of $0.007a$, $0.01a$, $0.02a$, and $0.05a$. Results with static disorder configurations were in good agreement with computer simulations.

Before studying the localization effects, we first verified Bloch-wave behavior by making measurements with the masses spaced periodically. The frequency response (band structure) of the system was measured by our monitoring the transverse wave amplitude near one end of the series of masses while sweeping the frequency (analogous to electron Fermi energy) of the transverse actuator at the opposite end. Results for the second pass band (which corresponds to fitting approximately one-half transverse wavelength between the masses) are shown in Fig. 2(a). The response shows distinct edges separating the pass band from transmission gaps on ei-

ther side and approximately fifty eigenfrequencies corresponding to the eigenstates of the fifty-site system. The two internal regions of low response, as well as slow variations in the eigenstate amplitudes, may be attributed to the $\sim 13\%$ variation in the sizes of the commercial lead masses. The band is fairly narrow, extending from about 760 to 840 Hz. All the eigenstates have about the same lifetime, $\tau = 0.9 \pm 0.1$ s. If the longitudinal strain modulation is applied to the periodic system, states corresponding to distinct one-, two-, etc., phonon processes appear in the gaps. By driving the static periodic system at one of the eigenfrequencies and translating the magnet, we record a Bloch-wave eigenstate; two examples are presented in Figs. 3(a) and 3(b), which show the eigenstate amplitude as a function of position along the wire. These eigenstates are clearly extended, and are in qualitative agreement with theoretical Bloch eigenstates.

The inelastic-scattering measurements were made with 2% disorder, i.e., with the masses displaced from the periodic lattice sites with a flat random distribution between $\pm 0.02a$. The frequency response of a static disordered configuration is shown in Fig. 2(b), which illustrates the dramatic departure from the Bloch response in Fig. 2(a). At least one eigenstate appears in the low-frequency gap. Eigenstates corresponding to various peaks in Fig. 2(b) are shown in Figs. 3(c)–3(g). The

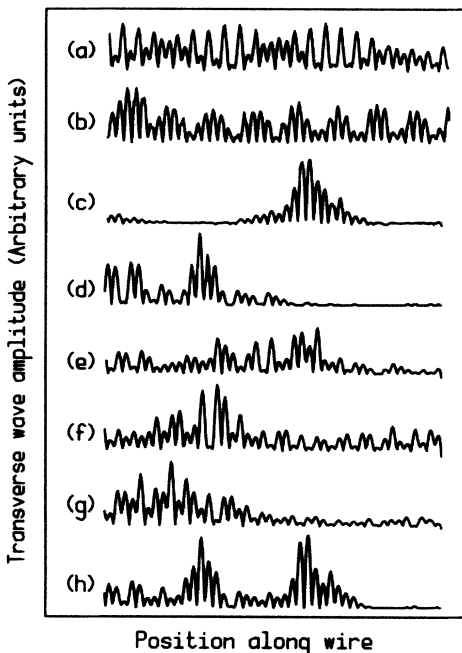


FIG. 3. Eigenstate amplitude as a function of position along the wire. (a), (b) Bloch-wave states. (c)–(g) Eigenstates of the 2% disordered system. (h) Mixing of states c and d due to the time-dependent potential. The sharp minima in the amplitude [~ 45 shown in (b)] indicate the positions of the masses, spaced at the lattice constant $a = 15$ cm.

most localized state, Fig. 3(c), was the low-frequency gap state in Fig. 2(b). The eigenstate in Fig. 3(d) was located approximately at the original Bloch band edge, and the other eigenstates in Figs. 3(e)–3(g) were inside the band. The eigenstates in Figs. 3(c) and 3(d) were remeasured with a logarithmic amplifier, and linear fits to this data indicated localization lengths of $(2.2 \pm 0.3)a$ and $(3.8 \pm 0.3)a$, respectively.

For the inelastic-scattering measurements one of the eigenstates in Figs. 3(c)–3(g) was selected as an initial state $|i\rangle$, and another was chosen as a final state $|f\rangle$. The transverse actuator was driven at the initial-state eigenfrequency ω_i , and the longitudinal actuator was driven at the frequency for resonant phonon-assisted hopping, $\Omega = |\omega_i - \omega_f|$. The response of the system, represented as a mixture $\alpha|i\rangle + \beta|f\rangle$, was then measured as a function of the amplitude of the longitudinal strain modulation ϵ . Steady-state response consisted of energy being transferred back and forth between the two states $|i\rangle$ and $|f\rangle$ at the frequency Ω . The time average of the mixture for a particular longitudinal strain amplitude is shown in Fig. 3(h). If the actuators were stopped, energy would be transferred to the final state with a hopping probability of $|\beta/\alpha|^2$. A plot of the measured hopping probability as a function of the longitudinal drive amplitude is presented in Fig. 4, where the initial and final states were those of Figs. 3(d) and 3(e), respectively. Other pairs of states, *dc*, *fe*, *fc*, *ge*, and *gc*, where the letters refer to Fig. 3, gave similar plots, but with widely varying vertical scales (to be discussed below).

For convenience in comparing our data with other Anderson localization systems, we have converted the longitudinal strain modulation amplitude ϵ to a normalized (dimensionless) inelastic-scattering rate. From Ziman,¹² an electron-phonon scattering rate may be given as

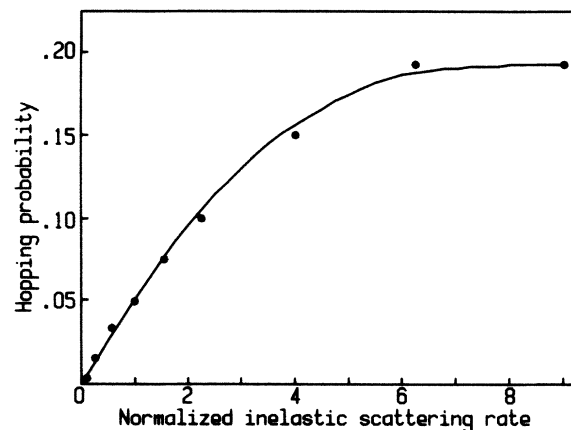


FIG. 4. Hopping probability as a function of strain amplitude, expressed as a normalized inelastic-scattering rate (see text).

$S = (2\pi/\hbar) |\epsilon \partial E / \partial \epsilon|^2 \rho(E)$, where the deformation potential $\partial E / \partial \epsilon$ is the rate of change of a system eigenvalue E with a static strain ϵ and $\rho(E)$ is the density of states. We assume that $1/\rho(E) = \Delta E$, the average separation between eigenvalues, and define the normalized inelastic-scattering rate as $s = \hbar S / \Delta E = 2\pi |(\epsilon / \Delta E) \partial E / \partial \epsilon|^2$. For our acoustic system $s = 2\pi |(\epsilon / \Delta \omega) \partial \omega / \partial \epsilon|^2$, where the eigenfrequency spacing $\Delta \omega$ and the eigenfrequency shift $\partial \omega / \partial \epsilon$ are measured directly. It should be noted that interesting behavior should occur when $\epsilon \partial \omega / \partial \epsilon \sim \Delta \omega$, or when $s \sim 2\pi$; at this point the strain causes the eigenfrequencies of neighboring states to coincide with that of the initial state. In Fig. 4 it can be seen that the resonant phonon-assisted hopping becomes nonlinear when $s > 1$, and saturates when $s > 2\pi$.

In the region $s < 1$ the hopping probability is linearly related to the longitudinal strain amplitude squared, and we have attempted an analysis using first-order time-dependent perturbation theory. The theory requires evaluation of the matrix element $\langle f | \partial V / \partial \epsilon | i \rangle$, and this is difficult to do in detail. It is usually assumed¹⁰ that for localized states the overlap is dominated by the exponential decay of the eigenstate amplitudes. Motivated by this we write $|\langle f | \partial V / \partial \epsilon | i \rangle|^2 = |\partial E / \partial \epsilon|^2 A \Phi$, where

$$A = \left(\int |\psi_f(x)| |\psi_i(x)| dx \right)^2 \quad (2)$$

and Φ is a correction due to the contribution of the phases of the eigenstates in the matrix element. The usual assumption corresponds to $\Phi = \text{const}$ (i.e., Φ is fixed by an averaging over some assumed random distribution of phases¹⁰).

From first-order time-dependent perturbation theory we find $|\beta/\alpha|^2 = (2/\pi)(\Delta\omega\tau)^2 A \Phi s$. By comparing this expression with the linear region of our plots of hopping probability versus s , and with A in Eq. (2) determined from our recorded data, we can obtain values for Φ . For the six pairs of eigenstates dc , fc , gc , de , fe , and ge from Fig. 3, Φ is found to be (0.21, 0.028, 0.016, 0.43, 0.31, and 0.004) $\times 10^{-3}$, respectively. The small values of Φ indicate that the operator $\partial V / \partial \epsilon$ weakly couples the orthogonal eigenstates $|i\rangle$ and $|f\rangle$. From the large fluctu-

ations in Φ for the different pairs of states we conclude that a constant random-phase correction is a poor approximation; the large variations in the scale of $|\beta/\alpha|^2$ cannot be wholly accounted for with the variations in A . At least in the case where the phonon wavelength is larger than the localization length, the phase as well as the amplitude overlap strongly influences the hopping rate. Local phase correlation and the restriction of the overlap integral to a limited region of space may make the eigenstate phase an important factor. More studies of the effects of phase correlation between different localized eigenstates would be of interest.

Stimulating and helpful discussions with D. Browne, J. Sethna, and D. DiVincenzo of Cornell University are gratefully acknowledged. This work was supported by National Science Foundation Grant No. DMR 8304371 and by the U.S. Office of Naval Research.

¹P. W. Anderson, Phys. Rev. **109**, 1492 (1958).

²N. F. Mott, Adv. Phys. **16**, 49 (1967).

³A. B. Fowler, G. L. Timp, J. J. Wainer, and R. A. Webb, Phys. Rev. Lett. **57**, 138 (1986).

⁴G. J. Dolan, J. C. Licini, and D. J. Bishop, Phys. Rev. Lett. **56**, 1493 (1986).

⁵M. J. Stephen, Phys. Rev. Lett. **56**, 1809 (1986).

⁶S. John, H. Sompolinsky, and M. J. Stephen, Phys. Rev. B **27**, 5592 (1983); M. L. Williams and H. J. Maris, Phys. Rev. B **31**, 4508 (1985).

⁷S. Cohen and J. Machta, Phys. Rev. Lett. **54**, 2242 (1985); C. A. Condat and T. R. Kirkpatrick, Phys. Rev. B **32**, 495 (1985).

⁸P. A. Lee and A. D. Stone, Phys. Rev. Lett. **55**, 1622 (1985).

⁹Local time-dependent potentials have been treated by A. D. Stone, M. Ya. Azbel, and P. A. Lee, Phys. Rev. B **31**, 1707 (1985). See also A. D. Stone and P. A. Lee, Phys. Rev. Lett. **54**, 1196 (1985).

¹⁰N. F. Mott, Philos. Mag. **19**, 835 (1969).

¹¹M. Ya. Azbel, Phys. Rev. B **28**, 4106 (1983).

¹²J. M. Ziman, *Electrons and Phonons* (Clarendon, London, 1960).

¹³K. Ishii, Prog. Theor. Phys. Suppl. **53**, 77 (1973).